

In Vivo Intravascular Ultrasound-Based 3D Thin-Walled Model for Human Coronary Plaque Progression Study: Transforming Research to Potential Commercialization

*Jian Guo,¹ Liang Wang,² David Molony,³ Habib Samady,³ Jie Zheng,⁴ Xiaoya Guo,⁵ Akiko Maehara⁶, Gary S. Mintz⁶, Jian Zhu,⁷ †Genshan Ma,⁷ †Dalin Tang^{1,2}

¹School of Biological Science & Medical Engineering, Southeast University, Nanjing, China

²Mathematical Sciences Department, Worcester Polytechnic Institute, Worcester, MA 01609 USA

³Department of Medicine, Emory University School of Medicine, Atlanta, GA, 30307, USA

⁴Mallinckrodt Institute of Radiology, Washington University, St. Louis, MO, 63110, USA

⁵Department of Mathematics, Southeast University, Nanjing, 210096, China

⁶The Cardiovascular Research Foundation, Columbia University, New York, NY 10022, USA

⁷Department of Cardiology, Zhongda Hospital, Southeast University, Nanjing, 210009, China

* Presenting author: Jian Guo, School of Biological Science & Medical Engineering, Southeast University, Nanjing China, email: wyguojian@126.com.

† Corresponding authors. (1) Dalin Tang, Mathematical Sciences Department, Worcester Polytechnic Institute, Worcester, MA 01609, email: dtang@wpi.edu; (2) Genshan Ma, Department of Cardiology, Zhongda Hospital, Southeast University, Nanjing, 210009, China, magenshan@hotmail.com.

Abstract

Cardiovascular disease (CVD) is the leading cause of death in the world. Considerable research has been done linking various risk factors to plaque progression and rupture which often lead to drastic clinical events such as heart attack and stroke. However, methods transforming research results to clinical implementation are limited. There has been evidence indicated that mechanical stress and strain may be linked to plaque progression. However, 3D plaque model construction is extremely time consuming making it near impossible for clinical implementations. 2D structure-only model is easy to make, but its stress/strain predictions are not good enough to serve as approximation to 3D solutions. In this study, an in vivo IVUS based 3D Thin-Wall model was developed to approximate 3D FSI model for clinical implementations. Results from one patient data (100 TW models) indicated that mean value of maximum plaque wall stress (MPWS) and average plaque wall stress (APWS) from TW model were 1.9% and 3.0% higher than those from FSI model (MPWS: 127.2 ± 74.3 kPa vs. 124.8 ± 65.7 kPa, APWS: 65.9 ± 18.8 kPa vs. 64.0 ± 21.4 kPa). Mean value of maximum plaque wall strain (MPWSn) and average plaque wall strain (APWSn) from TW model were 1.3% and 1.6% lower than those from FSI model (MPWSn: 0.0760 ± 0.0221 vs. 0.0770 ± 0.0161 , APWSn: 0.0572 ± 0.0056 vs. 0.0581 ± 0.0070). Wall thickness (WT) from TW model was 1.7% lower than those from FSI model (0.0630 ± 0.0126 cm vs. 0.0640 ± 0.0126). At baseline, PWS and plaque progression measured by wall thickness increase (WTI) had no significant correlations using either FSI or TW models (FSI: $r = 0.0446$, $p = 0.7684$; TW: $r = -0.0414$, $p = 0.7848$). WT had significant negative correlation with WTI (FSI: $r = -0.3337$, $p = 0.0234$; TW: $r = -0.3559$, $p = 0.0152$). PWSn had weak positive correlation with WTI by FSI model ($r = 0.2830$, $p = 0.0506$), while this cannot be predicted by TW model ($r = -0.1493$, $p = 0.3219$). Large scale studies are needed to further investigate the feasibility of using TW models as approximation for FSI models in potential clinical implementations.

Key words: Coronary, fluid-structure interactions, plaque progression, vulnerable plaque, IVUS.

1. Introduction

Cardiovascular disease (CVD) is the leading cause of death in the world. It is well known that most of the heart attacks are related to the rupture of vulnerable plaques [1][12]. However, it has been a great challenge to understand the mechanisms governing plaque progression and rupture and predict them before tragical clinical events happen. Interventional surgical treatments such as stenting, carotid endarterectomy (CEA), and graft bridging are routinely used in CVD treatment with artery stenosis severity used as the primary guidance. On the other hand, it has been well documented that stenosis severity does not correlate well with occurrence of CVD clinical events calling for surgical interventions [16][24]. Considerable effort has been devoted to identify possible linkage between mechanical stress/strain conditions and plaque progression and rupture. Since 3D model construction is time consuming, that became a hinder in bringing modeling research results to real clinical applications. In this paper, we demonstrate that 3D thin-walled models could serve as a tool to overcome that difficulty.

Plaque progression and rupture are complex processes involving many factors including mechanical forces, plaque morphology, hemorrhage, cell activities, blood conditions and many others. And it is well believed that the mechanical factors play an important role. With the improvement of medical imaging, many research groups have proposed and improved the computational models based on the clinical image data to obtain more accurate and reliable plaque stress/stain and flow shear stress conditions. The mature one was the multi-component Fluid-Structure Interaction (FSI) model based on the in vivo data [28], which was validated by experimental data on its accuracy and reliability [4][19][22]. As mentioned above, the model construction time limited its application for clinical implementations. Considering other alternatives, 2D structure model could not provide more reliable result, while 3D wall-only model did not reduce the model constructing and solving time [8][26]. Recently, a new thin layer structure only model (TLS) based on ex vivo MR-Image data was introduced, the results from TLS model showed good agreement with FSI model, and the time of model constructing and solving was controlled within 2 hours per plaque, which provided the possibility of its use for clinical plaque assessment [7].

In this paper, thin-wall (TW) and FSI models were constructed based on patient follow-up intravascular ultrasound (IVUS) for a patient. Plaque stress, strain and wall thickness data from both models were compared to find the differences and seek the feasibility of using TW models to replace 3F FSI models for potential clinical applications. Results for plaque progression correlation analysis from both models were also compared.

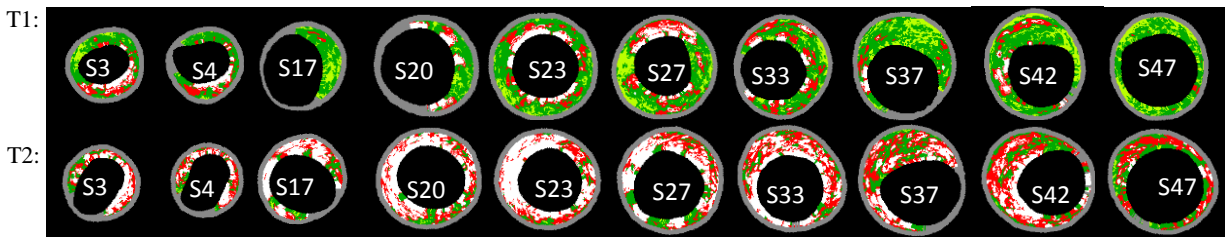
2. Method

2.1 IVUS data acquisition

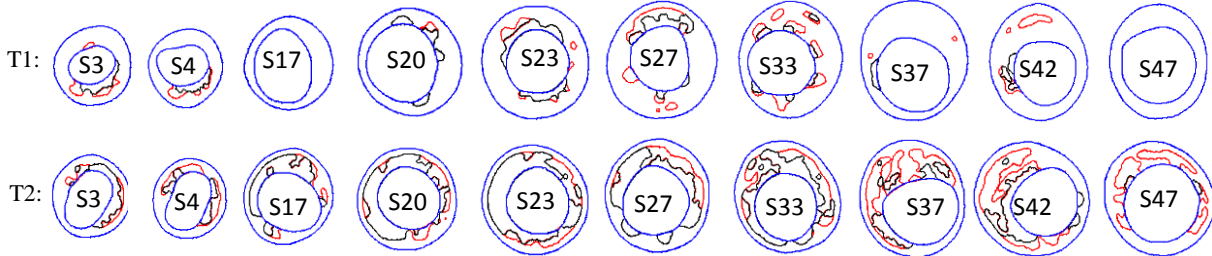
Patient follow-up IVUS data of coronary plaques from one patient (Gender: M, Age: 52) were provided by Cardiovascular Research Foundation (Cardiovascular Research Foundation, New York, United States) with informed consent obtained at time of data acquisition. Vessel and multi-components detection was performed to obtain IVUS-VH (Virtual Histology) data using automated Virtual Histology software (version 3.1) on a Volcano s5 Imaging System (Volcano Crop., Rancho Cordova, CA). IVUS-VH slices at the baseline (T1) and follow-up (T2) were processed to obtain contours for vessel lumen, out-boundary and plaque components for model construction using established procedures described in *Yang et al.* [28].

X-ray angiogram (Allura Xper FD10 System, Philips, Bothel, WA) was obtained at both baseline scan (T1) and follow-up scan (T2) prior to the pullback of the IVUS catheter to determine the location of the coronary artery stenosis, vessel curvature and cyclic bending caused by heart contraction. Fusion of angiography and IVUS slices was done using method similar to that described in *Wahle et al.* [25]. The view angle of the angiography was chosen so that the angiography plane was close to the principal tangent plane of the chosen coronary segment. Co-registration (both longitudinal and circumferential) of baseline and follow-up IVUS data were performed by IVUS expert using angiography movie, location of the myocardium, vessel bifurcation, stenosis and plaque component features. Figure 1 gives the patient follow-up IVUS images, contours and reconstructed 3D geometry of the plaque.

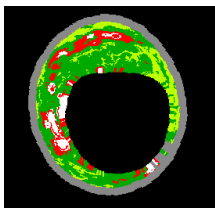
(a) Selected IVUS slices from 55 model slices matched at baseline (T1) and follow up (T2)



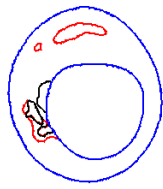
(b) Contour plots of selected slices matched at baseline (T1) and follow up (T2)



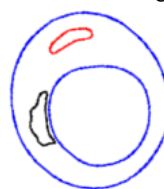
(c) Enlarged view



(d) Enlarged contour



(e) Enlarged contour after smoothing



(f) Re-constructed 3D plaque geometry

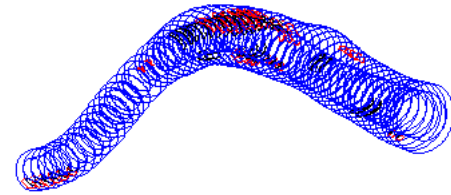


Figure 1. Patient follow-up IVUS data from a patient. (a) Baseline (T1) and follow up (T2) co-registered IVUS-VH and (b) segmented contours; (c) Enlarged view of S42; (d) Enlarged contour of S42; (e) Enlarged contour after smoothing; (f) Re-constructed 3D plaque geometry.

2.2 Pressure condition and material parameters

Patient-specific systolic and diastolic pressure was used to scale a typical coronary blood pressure profile obtained from catheterization and adopted in our model. Figure 2 shows the upstream pressure (P_{in}) and the downstream pressure (P_{out}) used in the 3D FSI model. Axial pressure drop was not needed in TW model which is structure-only and had no flow. The uniform pressure (P_{in}) was applied over the lumen surface of TW model.

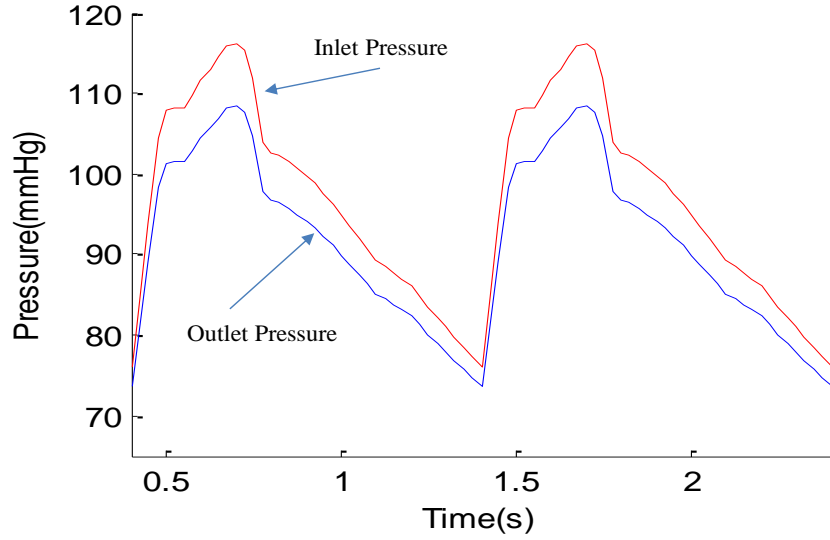


Figure 2. The cardiac pressure profile used for the FSI and TW models.

Vessel material was assumed to be hyperelastic, anisotropic, nearly-incompressible and homogeneous. Plaque components were assumed to be hyperelastic, isotropic, nearly incompressible and homogeneous for simplicity. No-slip conditions and natural traction equilibrium conditions were assumed at all interfaces. Our complete FSI model can be found from *Yang et al.* and are omitted here [28].

Biaxial testing was performed using eight coronary arteries from 4 cadavers (age: 50-81) to obtained realistic vessel material data for our model [9]. A modified Mooney-Rivlin model was used for the vessel fitting our biaxial data: [9][28]

$$W = c_1(I_1 - 3) + c_2(I_2 - 3) + D_1[\exp(D_2(I_1 - 3)) - 1] + K_1/(2K_2) \exp[K_2(I_4 - 1)^2 - 1] \quad (1)$$

$$I_1 = \sum C_{ii}, \quad I_2 = 1/2[I_1^2 - C_{ij}C_{ij}] \quad (2)$$

where I_1 and I_2 are the first and second invariants of right Cauchy-Green deformation tensor \mathbf{C} defined as $\mathbf{C} = [C_{ij}] = \mathbf{X}^T \mathbf{X}$, $\mathbf{X} = [X_{ij}] = [\partial x_i / \partial a_j]$ (x_i) is current position, (a_i) is original position), $I_4 = C_{ij}(n_c)_i(n_c)_j$, n_c is the unit vector in the circumferential direction of the vessel, $c1$, $D1$, $D2$, and $K1$ and $K2$ are material constants. The parameter values used in this paper were: $c1 = -1312.9$ kPa, $c2 = 114.7$ kPa, $D1 = 629.7$ kPa, $D2 = 2.0$, $K1 = 35.9$ kPa, $K2 = 23.5$. Our measurements are also consistent with data available in the literature [2][3][23][26][27].

2.3 Plaque geometry reconstruction and computational models

About plaque geometry reconstruction, several important techniques and details should be explained. First, since arteries were axially stretched and pressurized under in vivo condition, a preshrink ratio should be found to shrink the in vivo shape to a no-load shape so that when axial stretch and pressure were added, the artery could re-gain its in vivo shape [4]. Second, cyclic bending of coronary arteries caused by cardiac contraction/expansion should be involved in the 3D FSI model to obtain more accurate result. Another major step to construct the computational model was the mesh generation, and the Volume Component-Fitting Method was applied to

generate mesh for the plaque models [5][28]. In that process, the plaque was divided into hundreds of small volumes to curve-fit the complex plaque geometry, and to generate mesh for the finite element model which will be solved by ADINA (Adina R & D, Watertown, MA).

The thin-wall (TW) model was made by adding a thin wall thickness to a plaque slice to form a 3D model. Since the TW model does not really have 3D geometry complications, mesh generation is practically the same as 2D models. There were no cyclic bending and fluid part for it. However, compared to 2D structure only models, axial stretch was included in TW model. In this way, TW model reserved some characteristics of 3D model and greatly simplified the complexity of model construction. Figure 3 showed the construction process of TW model.

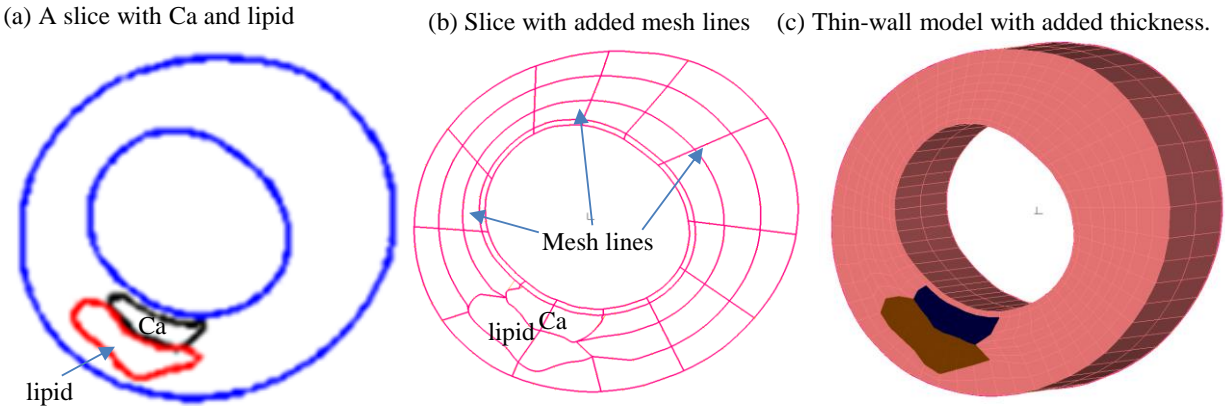


Figure 3. The process of constructing a TW model. (a) A slice with Ca and lipid; (b) Slice with added mesh line; c) Thin-wall model with added thickness.

2.4 Finite element simulation and solution method

The computational models were solved using the commercial finite package ADINA (ADINA R&D Inc., USA), which offers a wide range of capabilities based on reliable and efficient finite element procedures. The governing finite element equations were solved by the modified Newton-Raphson iteration method. More details of the computational models and solution methods can be found in *Tang et al.* [4][17].

2.5 Data analysis

Plaque wall stress (PWS), strain (PWSn), and wall thickness (WT) values were extracted from the solutions from 3D FSI and TW models for analysis. The maximum principal stress and maximum principal strain were used as the scalar values of plaque stress and strain for simplicity. Results on matched lumen nodes from TW model and FSI model were compared to investigate their differences. Using the FSI model results as the bench mark, the relative error of the TW model is defined as:

$$Error = \frac{1}{n} (\sum_{i=1}^n |a_i - b_i|/b_i) \quad (3)$$

where a_i was the values from TW models, b_i was the values from FSI models, and n was the number of data points.

For progression analysis, slices at baseline (T1) and follow up (T2) were paired. Plaque progression was measured by wall thickness increase (WTI) defined as WT at T2 – WT at T1. Correlation results using FSI models and TW models were compared.

3. Results

3.1 Construction time

Technically, TW 3D model is expanded from 2D model. The cost of time on model constructing and solving for a TW model is almost same as that for a 2D model. However, when it comes to FSI model, 3D wall only-model or TLS model, because all of them are 3D models in nature, the cost of time would obviously be more than that for TW model.

For an experienced researcher, it takes less than 10 minutes to perform all steps for one TW model. For the case we are using, there are 50 slices. So 50 TW models took less than 10 hours to construct and obtain all the results. On the other hand, construction for one FSI model or 3D wall-only model normally takes 1-2 week (for a trained operator), which makes it impossible for potential clinic implementations.

3.2 Comparisons of TW models and FSI models on plaque wall stress/strain, and wall thickness

Figure 4 gives mean value bar plots of plaque wall strain (PWSn) at T1 and T2 from FSI and TW models showing comparisons. Table 1 shows plaque wall stress (PWS), plaque wall strain (PWSn), and wall thickness (WT) from FSI and TW models. Mean value of MPWS and APWS from all TW models (100 models) were 1.9% and 3.0% higher than those from FSI model (MPWS: 127.2 ± 74.3 kPa vs. 124.8 ± 65.7 kPa, APWS: 65.9 ± 18.8 kPa vs. 64.0 ± 21.4 kPa). with relative errors were 11.9% and 6.7%, respectively. And mean value of MPWSn and APWSn from all TW models (n=100) were 1.3% and 1.6% lower than those from FSI model (MPWSn: 0.0760 ± 0.0221 vs. 0.0770 ± 0.0161 , APWSn: 0.0572 ± 0.0056 vs. 0.0581 ± 0.0070). Their relative errors were 10.5% and 4.9%.

With regard to WT, TW models showed good agreement with FSI models. The mean value of WT obtained from TW models was 1.7% lower than that from FSI model (0.0630 ± 0.0126 cm vs. 0.0640 ± 0.0126), and the relative errors was 1.7%.

Overall results suggested that the values of various factors provided by TW model had slight differences with those by FSI model, most of them kept the relative error lower than 10%.

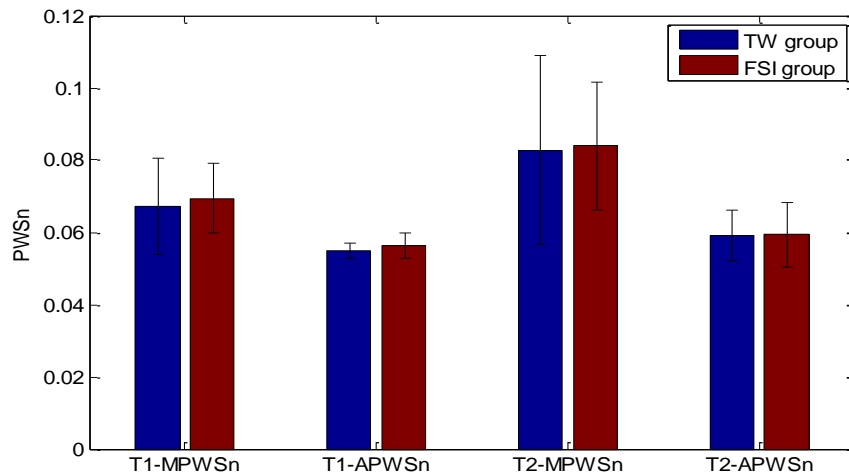


Figure 4. Comparison of PWSn between TW model and FSI model at baseline (T1) and follow up (T2).

Table.1 The comparison of PWS, PWSn and WT between FSI model and TW model

Factors	Period	Slices	TW	FSI	Error(%)
MPWS(kPa)	T1	49	97.4±37.2	94.5±24.4	11.3
	T2	50	150.5±89.3	150.7±78.1	13.3
	combined	92	127.2±74.3	124.8±65.7	11.9
APWS(kPa)	T1	49	59.9±6.8	57.5±6.3	5.6
	T2	50	70.0±24.9	68.6±28.5	8.3
	combined	92	65.9±18.8	64.0±21.4	6.7
MPWSn	T1	49	0.0671±0.0134	0.0694±0.0096	9.6
	T2	50	0.0828±0.0261	0.0840±0.0177	12.2
	combined	92	0.0760±0.0221	0.0770±0.0161	10.5
APWSn	T1	49	0.0549±0.0021	0.0564±0.0036	4.3
	T2	50	0.0591±0.0070	0.0593±0.0090	5.5
	combined	92	0.0572±0.0056	0.0581±0.0070	4.9
WT(cm)	T1	49	0.0636±0.0131	0.0640±0.0127	0.7
	T2	50	0.0628±0.0120	0.0645±0.0121	2.7
	combined	92	0.0630±0.0126	0.0640±0.0126	1.7

Combined data was based on the paired slice (92). Values are expressed as mean±standard deviation.

3.3 Correlation results between plaque progression (WTI) and risk factors using TW models and FSI models

Table 2 summarized the correlation results between plaque progression and three risk factors (PWS, PWSn, & WT) at baseline and follow up. At baseline, PWS and WTI had no significant correlations (FSI: $r = 0.0446$, $p = 0.7684$; TW: $r = -0.0414$, $p = 0.7848$). WT had significant negative correlation with WTI (FSI: $r = -0.3337$, $p = 0.0234$; TW: $r = -0.3559$, $p = 0.0152$). PWSn had weak positive correlation with WTI by FSI model ($r = 0.2830$, $p = 0.0506$), while this cannot be predicted by TW model ($r = -0.1493$, $p = 0.3219$).

The correlations by TW models were coincident with those by FSI models at follow up, there were no correlations between WT and WTI in both models (FSI: $r = 0.0806$, $p = 0.5945$; TW: $r = 0.0423$, $p = 0.7804$). PWS showed negative correlation with WTI in both models, but the TW model was weaker and not that significant (FSI: $r = -0.3718$, $p = 0.0109$; TW: $r = -0.2246$, $p = 0.1335$). The PWSn was in the same situation as PWS (FSI: $r = -0.3904$, $p = 0.0073$; TW: $r = -0.2358$, $p = 0.1147$).

Table 2. Correlation results between plaque progression (WTI) and the risk factors (PWS, PWSn, & WT) using FSI model and TW model at baseline(T1) and follow up(T2)

Model	Factors	T1(baseline)		T2(follow up)	
		r	p	r	p
FSI	PWS	0.0446	0.7684	-0.3718	0.0109
	PWSn	0.2830	0.0506	-0.3904	0.0073
	WT	-0.3337	0.0234	0.0806	0.5945
TW	PWS	-0.0414	0.7848	-0.2246	0.1335
	PWSn	-0.1493	0.3219	-0.2358	0.1147
	WT	-0.3559	0.0152	0.0423	0.7804

4. Discussion

4.1 Comparison with others modeling schemes

The comparisons of various risk factors to plaque progression between TW model and FSI model were reported in this paper. The relative errors of maximum PWS and PWSn using TW model data were slightly more than 10%, while the relation errors of the average PWS and PWSn were only about 5% in two cases. And it had much better performance in WT comparison. Those results indicated the TW model was better than 2D structure only model which had more than 30% relation error of PWS and PWSn [26].

TW models were in vivo IVUS based model, consequently, location specific pre-shrink ratio needed to be applied to for each slice. And there would be obvious differences between the results from TW model and those from FSI model in a small number of slices. As for TLS model based on the ex vivo data, due to the procedure without pre-shrink and the difference of model constructing the results of MPWS from TLS were closer to those from FSI model for each slice [7]. But overall statistical results, the accuracy of PWS from TW model was no less than it of TLS model.

4.2 TW models could be proper to be used for patient screening strategies.

Thin-Walled model involve the axial stretch to improve the accuracy and the time-saving characteristic is reserved comparing to 2D structure only model. What's more, TW model shorten the total time to several minutes, while there are still one or two hours needed to construct a TLS model. Since the TW model was expanded from 2D model, basically, the complexity to construct a TW model is almost same with that of a 2D model.

And it gives more possibility to finish the whole process automatically. From this demand, TW models might be practical to replace FSI models for the future clinical events.

4.3 Limitations for the models

In fact, the IVUS-VH cannot provide the data accurate enough, especially when it comes to the cap-thickness level. It is a common thing that the components cross over the lumen by segmented contour. Once this occurs, we keep the cap with thickness about 50 micron manually based the well accepted 65 micron threshold value for cap thickness. And this issue depends on the development of medical imaging. More accurate computational model could be constructed based on more accurate image. The other one is the lack of 3D vessel curvature data to make the 3D model more accurate.

Another limitation is that TW model is based on the single slice. This is why the TW model saves a lot of time and consequently it brings some disadvantages. Since it is current slice only, TW model cannot involve the impact from neighboring slices.

And the patient-specific and tissue-specific material properties were not considered in both models.

5. Conclusion

In this paper, a comparative analysis study between TW models and FSI models was performed. It was shown that the cost of TW model construction and data analysis was much less than that of FSI models. Errors of plaque stress and strain between TW and FSI models were less than 10%. However, correlation analysis results did not provide good agreement between the two models. Large scale studies are needed to investigate the feasibility of using TW models as approximation for FSI models.

Acknowledgements. This research was supported in part by NIH grant NIH/NIBIB R01 EB004759 and a Jiangsu Province Science and Technology Agency grant BE2016785.

References

- [1] Fuster, V. (1999). The vulnerable atherosclerotic plaque: understanding, identification, and modification. *Cardiovascular Drugs and Therapy*, 13(4), 363-363.
- [2] Holzapfel, G. A., G. Sommer, and P. Regitnig. (2004). Anisotropic mechanical properties of tissue components in human atherosclerotic plaques. *Journal Of Biomechanical Engineering*, 126(5):657 - 665.
- [3] Holzapfel, G. A., Mulvihill, J. J., Cunnane, E. M., & Walsh, M. T. (2014). Computational approaches for analyzing the mechanics of atherosclerotic plaques: A review. *Journal Of Biomechanics*, 47(4), 859-869.
- [4] Huang, X. (2009). In Vivo MRI-based three-dimensional fluid-structure interaction models and mechanical image analysis for human carotid atherosclerotic plaques.
- [5] Huang, X., Yang, C., Canton, G., Ferguson, M., Yuan, C., & Tang, D. (2012). Quantifying Effect of Intraplaque Hemorrhage on Critical Plaque Wall Stress in Human Atherosclerotic Plaques Using Three-Dimensional Fluid-Structure Interaction Models. *Journal Of Biomechanical Engineering-Transactions Of The Asme*, 134(12),
- [6] Huang, X., Yang, C., Zheng, J., Bach, R., Muccigrosso, D., & Woodard, P. K., et al. (2013). Abstract 9424: coronary artery disease-related death may be associated with higher critical plaque wall stress: a multi-patient 3d fluid-structure interaction study comparing plaque wall stress, flow shear stress, and plaque burden as risk indicators. *Circulation*(22), A9424.
- [7] Huang, X., Yang, C., Zheng, J., Bach, R., Muccigrosso, D., Woodard, P. K., & Tang, D. (2016). 3D MRI-based multicomponent thin layer structure only plaque models for atherosclerotic plaques. *Journal Of Biomechanics*, 49(27):26-2733.
- [8] Huang, Y., Teng, Z., Sadat, U., Graves, M. J., Bennett, M. R., & Gillard, J. H. (2014). The influence of computational strategy on prediction of mechanical stress in carotid atherosclerotic plaques: Comparison of 2D structure-only, 3D structure-only, one-way and fully coupled fluid-structure interaction analyses. *Journal Of Biomechanics*, 47(14):1465-1471.
- [9] Kural, M. H., Cai, M., Tang, D., Gwyther, T., Zheng, J., & Billiar, K. L. (2012). Planar biaxial characterization of diseased human coronary and carotid arteries for computational modeling. *Journal Of Biomechanics*, 45(5), 790-798.
- [10] Cai, M., Yang, C., Kural, M. H., Bach, R., Muccigrosso, D., Yang, D., Zheng, J., Billiar, K. L., Tang, D. (2011). Intravascular Ultrasound (IVUS)-Based Computational Modeling and Planar Biaxial Artery Material Properties for Human Coronary Plaque Vulnerability Assessment. *International Conference on Computational Engineering and Sciences (online Journal)*, ICCES, vol.19, no.4, pp.97-104.
- [11] Mintz, G. S., Nissen, S. E., Anderson, W. D., Bailey, S. R., Erbel, R., Fitzgerald, P. J., & ... Winters, J. L. (2001). American College of Cardiology clinical expert consensus document on standards for acquisition, measurement and reporting of intravascular ultrasound studies (IVUS). *Journal Of The American College Of Cardiology*, 37(14):1478-1492.
- [12] Naghavi, M., Libby, P., Falk, E., Casscells, S., Litovsky, S., Rumberger, J., & ... Willerson, J. (n.d). From vulnerable plaque to vulnerable patient - A call for new definitions and risk assessment strategies: Part I. *Circulation*, 108(14), 1664-1672.
- [13] Nair, A., Kuban, B. D., Tuzcu, E. M., Schoenhagen, P., Nissen, S. E., & Vince, D. G. (2002). Coronary plaque classification with intravascular ultrasound radiofrequency data analysis. *Circulation*, 106(17), 2200.

- [14] Nair, A., Margolis, M. P., Kuban, B. D., & Vince, D. G. (2007). Automated coronary plaque characterisation with intravascular ultrasound backscatter: ex vivo validation. *Eurointervention Journal of Europer in Collaboration with the Working Group on Interventional Cardiology of the European Society of Cardiology*, 3(1), 113-20.
- [15] Nasu, K., Tsuchikane, E., Katoh, O., Vince, D. G., Virmani, R., & Surmely, J. F., et al. (2006). Accuracy of in vivo coronary plaque morphology assessment: a validation study of in vivo virtual histology compared with in vitro histopathology. *Journal of the American College of Cardiology*, 47(12), 2405-2412.
- [16] Rothwell, P., Gutnikov, S., & Warlow, C. (n.d). Reanalysis of the final results of the European Carotid Surgery Trial. *Stroke*, 34(2), 514-523.
- [17] Tang, D., Yang, C., Kobayashi, S., & Ku, D. N. (2004). Effect of a lipid pool on stress/strain distributions in stenotic arteries: 3-d fluid-structure interactions (fsi) models. *Journal of Biomechanical Engineering*, 126(3), 363-370.
- [18] Tang, D., Yang, C., Zheng, J., Woodard, P. K., Sicard, G. A., & Saffitz, J. E., et al. (2004). 3d mri-based multicomponent fsi models for atherosclerotic plaques. *Annals of Biomedical Engineering*, 32(7), 947.
- [19] Tang, D. (2006). Flow in Healthy and Stenosed Arteries. Wiley Encyclopedia of Biomedical Engineering.
- [20] Tang, D., Teng, Z., Canton, G., Hatsukami, T. S., Dong, L., & Huang, X., et al. (2009). Local critical stress correlates better than global maximum stress with plaque morphological features linked to atherosclerotic plaque vulnerability: an in vivo multi-patient study. *BioMedical Engineering OnLine*, 8(1), 15.
- [21] Tang, D., Yang, C., Kobayashi, S., Zheng, J., Woodard, P. K., & Teng, Z., et al. (2009). 3d mri-based anisotropic fsi models with cyclic bending for human coronary atherosclerotic plaque mechanical analysis. *Journal of Biomechanical Engineering*, 131(6), 061010.
- [22] Tang, D., Teng, Z., Canton, G., Yang, C., Ferguson, M., & Huang, X., et al. (2009). Sites of rupture in human atherosclerotic carotid plaques are associated with high structural stresses: an in vivo mri-based 3d fluid-structure interaction study. *Stroke*, 40(10), 3258.
- [23] Tang, D., Kamm, R. D., Yang, C., Zheng, J., Canton, G., Bach, R., & ... Yuan, C. (2014). Image-based modeling for better understanding and assessment of atherosclerotic plaque progression and vulnerability: Data, modeling, validation, uncertainty and predictions. *Journal Of Biomechanics*, 47(SI: Plaque Mechanics), 834-846. doi:10.1016/j.jbiomech.2014.01.012
- [24] Underhill, H. R., Hatsukami, T. S., Fayad, Z. A., Fuster, V., & Yuan, C. (2010). Mri of carotid atherosclerosis: clinical implications and future directions. *Nature Reviews Cardiology*, 7(3), 165-73.
- [25] Wahle, A., Prause, P. M., Dejong, S. C., & Sonka, M. (1999). Geometrically correct 3-d reconstruction of intravascular ultrasound images by fusion with biplane angiography--methods and validation. *IEEE Transactions on Medical Imaging*, 18(8), 686-699.
- [26] Wang, H., Wang, L., Zheng, J., Zhu, J., Maehara, A., & Yang, C., et al. (2015). Using 2d in vivo ivus-based models for human coronary plaque progression analysis and comparison with 3d fsi models. *Procedia Engineering*, 126(2), 451-455.
- [27] Wang, L., Wu, Z., Yang, C., Zheng, J., Bach, R., & Muccigrosso, D., et al. (2015). Ivus-based fsi models for human coronary plaque progression study: components, correlation and predictive analysis. *Annals of Biomedical Engineering*, 43(1), 107-21.
- [28] Yang, C., Bach, R. G., Zheng, J., & Ei Naqa, I. (2009). In vivo, ivus-based 3-d fluid-structure interaction models with cyclic bending and anisotropic vessel properties for human atherosclerotic coronary plaque mechanical analysis. *IEEE Transactions on Biomedical Engineering*, 56(10), 2420.